

OPTICAL PROPERTIES OF SILICON NANOCRYSTALS: A FIRST PRINCIPLES STUDY

SERDAR ÖĞÜT*, JAMES R. CHELIKOWSKY*, STEVEN G. LOUIE**

*Department of Chemical Engineering and Material Science, Minnesota Supercomputing Institute, University of Minnesota, Minneapolis, Minnesota 55455.

**Department of Physics, University of California at Berkeley, and Materials Science Division, Lawrence Berkeley National Laboratory, Berkeley, California 94720.

ABSTRACT

Ab initio quasiparticle gaps, self-energy corrections, exciton Coulomb energies, and optical gaps of Si nanocrystals are calculated using the higher-order finite difference pseudopotential method. The calculations are performed in real space on hydrogen-passivated Si clusters with diameters up to 30 Å (> 1000 atoms). The size-dependent self-energy correction is enhanced substantially compared to bulk, and quantum confinement and reduced electronic screening result in appreciable excitonic Coulomb energies. Calculated optical gaps are in very good agreement with absorption data from Si nanocrystals.

INTRODUCTION

Understanding the role of quantum confinement (QC) in altering optical properties of semiconductor materials with reduced dimensions is a problem of both technological and fundamental interest. In particular, the discovery of visible luminescence from porous Si [1] has focused attention on optical properties of confined systems. Although there is still debate on the exact mechanism of photoluminescence in porous Si, there is a great deal of experimental and theoretical evidence that supports the important role played by QC in producing this phenomenon [2, 3]. Excitations in confined systems, like Si quantum dots as the building blocks of porous Si, differ from those in extended systems due to QC. In particular, the components that comprise the excitation energies, such as quasiparticle and exciton binding energies change significantly with the physical extent of the system. So far, most calculations that model semiconductor quantum dots have been of an empirical nature [4 – 8] owing to major challenges to simulate these systems from first principles. While empirical studies have shed some light on the physics of optical excitations in semiconductor quantum dots, one often has to make assumptions and approximations that may or may not be justified. Efficient and accurate *ab initio* studies are necessary to achieve a better microscopic understanding of the size dependence of optical processes in semiconductor quantum dots.

The main problem regarding the use of empirical approaches for semiconductor quantum dots centers on the transferability of the bulk interaction parameters to the nanocrystalline environment. The validity of this assumption, which postulates the use of fitted bulk parameters in a size regime of a few nanometers, is not clear, and has been questioned in recent studies [9]. More specifically, QC-induced changes in the self-energy corrections, which may affect the magnitude of the optical gaps significantly, are neglected in empirical approaches by implicitly assuming a “size-independent” correction that corresponds to that of the bulk. It follows that a reliable way to investigate optical properties of quantum

dots would be to model them from first principles with no uncontrolled approximations or empirical data. However, there have been two major obstacles for the application of *ab initio* studies to these systems. First, due to large computational demand, accurate first principles calculations have been limited to small system sizes, which do not correspond to the nanoparticle sizes for which experimental data are available. Second, even accurate *ab initio* calculations performed within the local density approximation (LDA) suffer from the underestimate of the band gap [10].

With recent advances in electronic structure algorithms [11, 12] and computational platforms, and alternative formulations of the optical gaps suitable for confined systems, the above-mentioned challenges for *ab initio* studies of quantum dots can be overcome. The use of a new electronic structure algorithm, the higher-order finite difference pseudopotential method [11], implemented on massively parallel computational platforms allows us to model a cluster of more than 1,000 atoms in a straightforward fashion [13]. As for the second problem regarding the underestimate of the band gap due to LDA, the confined nature of the quantum dots makes it possible for an alternative formulation of the fundamental quasiparticle gaps.

CALCULATIONAL METHODS

Our calculations were performed in real space using the higher-order finite difference pseudopotential method [11]. Quantum dots were modeled by spherical bulk-terminated Si clusters passivated by hydrogens at the boundaries (Fig. 1). We used Troullier-Martins pseudopotentials [16] in nonlocal [17] and local forms for Si and H, respectively. All calculations were performed within LDA using the exchange correlation functional of Ceperley and Alder [18]. The kinetic energy in the finite difference expression was expanded up to twelfth order in the grid spacing h chosen to be 0.9 a.u. No change in the calculated gap values was found upon decreasing h to 0.75 a.u. The wavefunctions were required to vanish outside a spherical domain, which was at least 7.5 a.u. away from the last shell of Si atoms. The diagonalizations were performed using the generalized Davidson algorithm with dynamical residual tolerance. Typically, 10 to 15 diagonalizations were needed to obtain the self-consistent charge density irrespective of the size of the system. The Hartree potential was solved by discretizing the Poisson equation and matching the boundary potential with that of a multipole expansion of the charge density with angular momentum $l = 9$ to 20. We considered quantum dots containing 65 to 1,005 atoms requiring the self-consistent solutions of 100 to 1,700 eigenpairs. With the grid spacing and domain size chosen as described above, the Hamiltonian sizes ranged from 25,000 to 250,000. All calculations were performed on a Cray C-90, except for the three largest cases $\text{Si}_{293}\text{H}_{172}$, $\text{Si}_{525}\text{H}_{276}$, and $\text{Si}_{705}\text{H}_{300}$, which were run in parallel on a Cray-T3E machine. Parallel implementation was performed using MPI with a domain decomposition approach, in which the whole physical domain was mapped on to 48 to 128 processors. For the largest cluster $\text{Si}_{705}\text{H}_{300}$, the performance on 128 processors was near 30 GFlops.

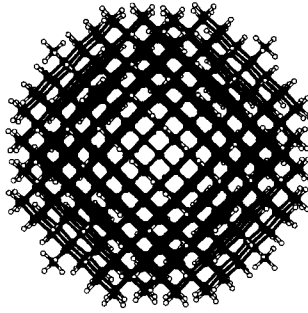


Figure 1: Atomic structure of a Si quantum dot with composition $\text{Si}_{525}\text{H}_{276}$. The gray and white balls represent Si and H atoms, respectively. This bulk-truncated Si quantum dot contains 25 shells of Si atoms and is 27.2 Å in diameter.

AB INITIO QUASIPARTICLE GAPS

For an n -electron system, the quasiparticle gap $\varepsilon_g^{\text{qp}}$ can be expressed in terms of the ground state total energies E of the $(n+1)-$, $(n-1)-$, and n -electron systems as

$$\varepsilon_g^{\text{qp}} = E(n+1) + E(n-1) - 2E(n) \quad (1)$$

$$= \varepsilon_g^{\text{HL}} + \Sigma, \quad (2)$$

where Σ is the self-energy correction to the HOMO-LUMO gap $\varepsilon_g^{\text{HL}}$ obtained within LDA. This definition is quite convenient for the calculation of the quasiparticle gap, as it is possible to excite individual electrons or holes from the ground state electronic configuration of a confined system. The calculation of $\varepsilon_g^{\text{qp}}$ requires the self-consistent solutions of three different charge configurations of each quantum dot. The computational demand of this approach can be reduced significantly by using the wavefunctions of the neutral cluster to extract very good initial charge densities for the self-consistent solutions of the charged systems. With a real-space method, total energies for charged $(n+1)-$ and $(n-1)-$ electron systems can be calculated in a straightforward fashion without the need for a compensating background charge that would be necessary for plane wave calculations with a supercell geometry.

Eq. (1) yields the correct quasiparticle gap $\varepsilon_g^{\text{qp}}$, if the *exact* exchange-correlation functional is used. Within LDA, in the limit of very large systems ($n \rightarrow \infty$), the gaps calculated using Eq. (1) approach the HOMO-LUMO gap $\varepsilon_g^{\text{HL}}$ [14]. However, for small systems, Eq. (1) captures the correction to the LDA HOMO-LUMO gap quite accurately (Table I) when compared with available GW calculations [15]. Small deviations appear as the system size reaches approximately 1,000 atoms in our calculations.

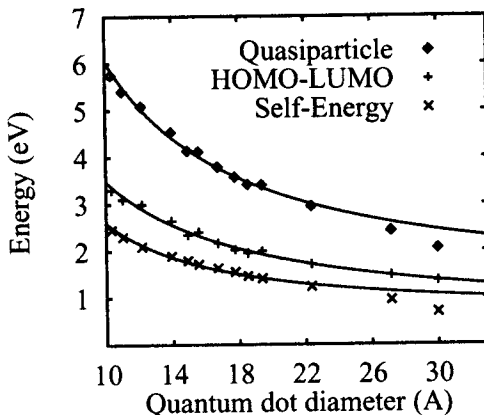


Figure 2: Calculated quasiparticle (\diamond) and HOMO-LUMO gaps ($+$), and self-energy corrections (\times) as a function of the quantum dot diameter d (in Å). The solid lines are power-law fits to the calculated data approaching the corresponding bulk limits. For small deviations from the fits for large system sizes, see the text.

The size dependence of the quasiparticle and LDA HOMO-LUMO gaps, and self-energy corrections are shown in Fig. 2. Both gap values and self-energy corrections are enhanced substantially with respect to bulk values, and are inversely proportional to the quantum dot diameter d as a result of QC. Specifically, $\varepsilon_g^{\text{qp}}(d) - \varepsilon_{g,\text{bulk}}^{\text{qp}}$, $\varepsilon_g^{\text{band}}(d) - \varepsilon_{g,\text{bulk}}^{\text{band}}$, and $\Sigma(d) - \Sigma_{\text{bulk}}$ scale as $d^{-1.2}$, $d^{-1.1}$, and $d^{-1.5}$, respectively. The quasiparticle gaps shown in Fig. 2 are significantly higher compared to the gap values obtained in earlier semi-empirical calculations [4 – 7]. The main reason for this is the significant enhancement of electron self-energies due to QC, which cannot be properly taken into account in semi-empirical approaches.

Table 1: HOMO-LUMO and quasiparticle gaps $\varepsilon_g^{\text{qp}}$ (Eq. 1) calculated for hydrogenated Si clusters compared to quasiparticle gaps calculated within the GW approximation [15]. All energies are in eV.

	$\varepsilon_g^{\text{HL}}$	$\varepsilon_g^{\text{qp}}$	GW
SiH ₄	7.9	12.3	12.7
Si ₂ H ₆	6.7	10.7	10.6
Si ₅ H ₁₂	6.0	9.5	9.8
Si ₁₄ H ₂₀	4.4	7.6	8.0

CALCULATIONS OF THE EXCITON COULOMB ENERGY

Since the quasiparticle gap refers to the energy needed to create a non-interacting electron-hole ($e-h$) pair, one cannot compare directly to measurements of the optical gap. This is a real issue for quantum dots in which the exciton radius becomes comparable to the size of the dot. QC in nanostructures enhances the bare exciton Coulomb interaction, and also reduces the electronic screening so that the exciton Coulomb energy E_{Coul} becomes comparable to the quasiparticle gap. Therefore, in order to extract the optical gaps $\varepsilon_g^{\text{opt}} = \varepsilon_g^{\text{qp}} - E_{\text{Coul}}$, the exciton Coulomb energy needs to be calculated accurately. Compared to E_{Coul} , exciton exchange-correlation energies are much smaller for the quantum dots studied in this work, and will therefore be neglected.

A crude, yet commonly used, approximation to E_{Coul} comes from the effective mass approximation (EMA) [19]. In the EMA, one assumes (i) an infinite potential barrier at the boundary of the quantum dot, and (ii) envelope wavefunctions of the form $\psi(\mathbf{r}) \sim \frac{1}{r} \sin(2\pi r)/d$ for a noninteracting $e-h$ pair. This yields (in a.u.) $E_{\text{Coul}} = 3.572/\epsilon d$. EMA, though commonly used, cannot be expected to yield accurate exciton Coulomb energies, since in this approximation the microscopic features of the electron-hole wavefunctions inside the quantum dot are neglected, and the wavefunctions are constrained to vanish abruptly outside the quantum dots, instead of decaying relatively slowly into the vacuum. We have, therefore, calculated E_{Coul} directly using *ab initio* pseudowavefunctions. The exciton Coulomb energy can be written as

$$\begin{aligned} E_{\text{Coul}} &= \int d\mathbf{r}_1 |\psi_e(\mathbf{r}_1)|^2 V_{\text{scr}}^h(\mathbf{r}_1) \\ &= \int d\mathbf{r}_1 |\psi_e(\mathbf{r}_1)|^2 \int d\mathbf{r} \epsilon^{-1}(\mathbf{r}_1, \mathbf{r}) V_{\text{unscr}}^h(\mathbf{r}) \\ &= \iiint \epsilon^{-1}(\mathbf{r}_1, \mathbf{r}) \frac{|\psi_e(\mathbf{r}_1)|^2 |\psi_h(\mathbf{r}_2)|^2}{|\mathbf{r} - \mathbf{r}_2|} d\mathbf{r} d\mathbf{r}_1 d\mathbf{r}_2. \end{aligned} \quad (3)$$

In this expression, V_{scr}^h and V_{unscr}^h are screened and unscreened potentials due to the hole, ψ_e and ψ_h are the electron and hole wavefunctions, and ϵ^{-1} is the inverse of the microscopic dielectric matrix. If we formally define $\tilde{\epsilon}^{-1}$ as

$$\int \epsilon^{-1}(\mathbf{r}_1, \mathbf{r}) \frac{1}{|\mathbf{r} - \mathbf{r}_2|} d\mathbf{r} \equiv \tilde{\epsilon}^{-1}(\mathbf{r}_1, \mathbf{r}_2) \frac{1}{|\mathbf{r}_1 - \mathbf{r}_2|}, \quad (4)$$

then the exciton Coulomb energy can be written as

$$E_{\text{Coul}} = \iint \tilde{\epsilon}^{-1}(\mathbf{r}_1, \mathbf{r}_2) \frac{|\psi_e(\mathbf{r}_1)|^2 |\psi_h(\mathbf{r}_2)|^2}{|\mathbf{r}_1 - \mathbf{r}_2|} d\mathbf{r}_1 d\mathbf{r}_2. \quad (5)$$

First, we set $\tilde{\epsilon} = 1$, and calculated the unscreened E_{Coul} . The results are shown in Fig. 3 along with the predictions of the EMA and recent empirical calculations [20]. The *ab initio* and empirical calculations for the unscreened Coulomb energy are in quite good agreement with each other, both predicting smaller Coulomb energies and a softer power-law decay compared to the EMA. In particular, fitting the calculated data to a power law of the diameter as $d^{-\beta}$, we find $\beta = 0.7$.

An accurate calculation of E_{Coul} requires the inverse dielectric matrix $\tilde{\epsilon}^{-1}(\mathbf{r}_1, \mathbf{r}_2)$ in Eq. (5). However, *ab initio* calculation of $\tilde{\epsilon}^{-1}(\mathbf{r}_1, \mathbf{r}_2)$ is computationally very demanding.

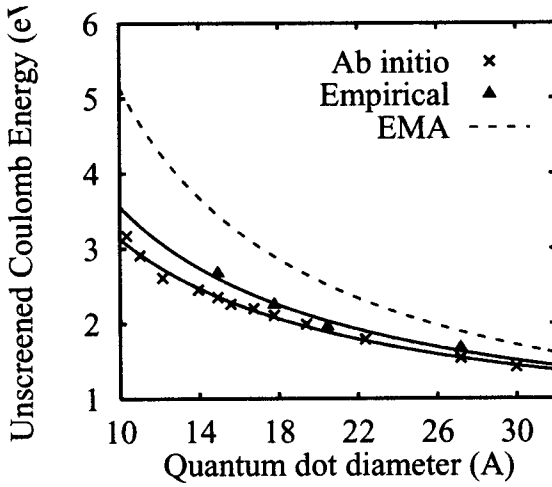


Figure 3: Unscreened exciton Coulomb energies as a function of the quantum dot diameter d (in Å) calculated by (i) effective mass approximation (dashed line), (ii) direct empirical pseudopotential calculations (Δ from Ref. [20]), (iii) direct *ab initio* pseudopotential calculations (\times) as explained in the text. The solid lines are power-law fits to the calculated data.

Earlier calculations used either the bulk dielectric constant or the reduced dielectric constant of the quantum dot for all $e-h$ distances. These are quite crude approximations, since the screening is different at different length scales due to the wavevector dependence of $\tilde{\epsilon}$. For example, when \mathbf{r}_1 and \mathbf{r}_2 in Eq. (5) are very close to each other, there will be practically no screening, and $\tilde{\epsilon} \approx 1$. Since both the hole and electron wavefunctions are well localized towards the center of the quantum dot, the screening will be reduced significantly, resulting in larger Coulomb energies compared to the case of using a single dielectric constant for all distances. We improve on these approximations by explicitly using the wavefunctions as calculated by our pseudopotential approach and a simplified, but realistic, dielectric function that takes spatial variations of $\tilde{\epsilon}$ into account.

To calculate the screening dielectric functions $\tilde{\epsilon}(\mathbf{r}_1, \mathbf{r}_2)$ of a particular quantum dot, we proceeded as follows: First, we applied spatially modulated electric fields at several wavevectors to calculate the q -dependent polarizability $\alpha(\mathbf{q})$ using a finite-field method. The q -dependent dielectric function $\tilde{\epsilon}(\mathbf{q})$ was then obtained using a dielectric sphere model [21]. The results for $\tilde{\epsilon}(\mathbf{q})$ of the $\text{Si}_{87}\text{H}_{76}$ quantum dot are shown in Fig. 4. After fitting the calculated $\tilde{\epsilon}(\mathbf{q})$ to a rational polynomial function of q and Fourier-transforming to real space [22], we obtained the dielectric function $\tilde{\epsilon}(r = |\mathbf{r}_1 - \mathbf{r}_2|)$. Implicitly, we are assuming spatial isotropy in writing $\tilde{\epsilon}(\mathbf{r}_1, \mathbf{r}_2) \approx \tilde{\epsilon}(r = |\mathbf{r}_1 - \mathbf{r}_2|)$. As shown in Fig. 4, the calculated $\tilde{\epsilon}(\mathbf{q})$ has a very sharp drop to ≈ 1 beyond $q = 0.2$ a.u., which corresponds

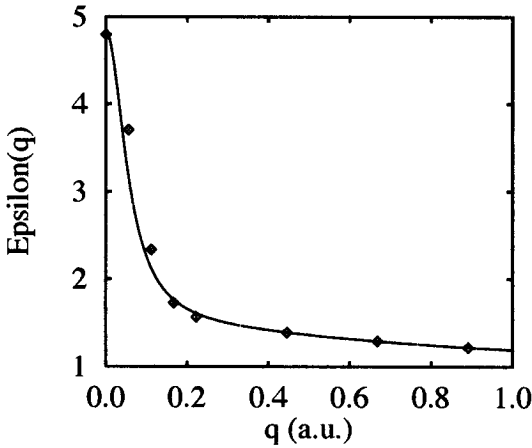


Figure 4: Wavevector dependence of the dielectric function for the $\text{Si}_{87}\text{H}_{76}$ quantum dot.

roughly to the wavevector set by the linear dimension (or diameter) of this quantum dot. In fact, this sharp drop is typical for all quantum dots studied. In real space, this implies that the $e - h$ interaction is very inefficiently screened inside the dot. This results in substantial excitonic Coulomb energies.

OPTICAL GAPS AND COMPARISON TO EXPERIMENT

The resulting optical gaps $\epsilon_g^{\text{opt}} = \epsilon_g^{\text{qp}} - E_{\text{Coul}}$ along with the quasiparticle gaps and experimental absorption data [23] from Si:H nanocrystals are shown in Fig. 5. Although the calculated quasiparticle gaps are ~ 0.6 to 1.0 eV larger than the experimental absorption data, the calculated optical gaps are in excellent agreement with experiment. At this point, an interesting observation can be made about the good agreement of previous semi-empirical calculations with experiment [2, 4, 6]. In the above semi-empirical approaches, it is the underestimate of *both* the quasiparticle gaps *and* the exciton Coulomb energies (through the use of a static dielectric constant of either the bulk or the quantum dot), that puts the calculated values in good agreement with experiment. As a matter of fact, the bare gaps of Refs. [4] and [6] without the exciton Coulomb energies are in better agreement with the experiment. Our present results demonstrate that (i) the quasiparticle gaps in Si quantum dots are actually higher than previously thought, and (ii) the exciton Coulomb energies, because of the wavevector dependence of the dielectric response function $\epsilon(\mathbf{r}_1, \mathbf{r}_2)$, are higher than previously calculated, resulting in optical gap values that are in good agreement with the experimental absorption data.

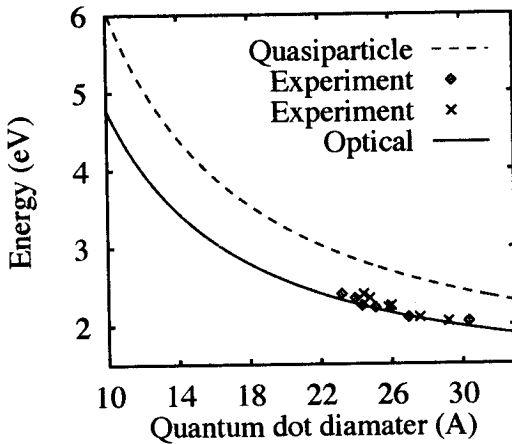


Figure 5: Calculated quasiparticle gaps (dotted line), optical gaps, and experimental absorption data from Si:H nanocrystals (\times and \diamond from Ref. [23]) as a function of the quantum dot diameter d (in Å). The two sets of experimental data (\times and \diamond) differ by the method to estimate the nanocrystal size.

ACKNOWLEDGMENTS

We thank J. Grossman, H. Kim, and I. Vasiliev for useful discussions, and A. Stathopoulos, Y. Saad, and B. Rackner for their help in implementing the finite-difference pseudopotential code on the T3E. We also acknowledge support for this work by the National Science Foundation and Minnesota Supercomputing Institute.

References

- [1] L. T. Canham, Appl. Phys. Lett. **57**, 1046 (1990).
- [2] D. J. Lockwood, Solid State Commun. **92**, 101 (1994).
- [3] M. V. Wolkin, J. Jorne, P. M. Fauchet, G. Allan, C. Delerue, Phys. Rev. Lett. **82**, 197 (1999).
- [4] J. P. Proot, C. Delerue, and G. Allan, Appl. Phys. Lett. **61**, 1948 (1992); C. Delerue, G. Allan, and M. Lannoo, Phys. Rev. B **48**, 11 024 (1993).
- [5] T. Takagahara and K. Takeda, Phys. Rev. B **46**, 15 578 (1992).
- [6] L. W. Wang and A. Zunger, J. Phys. Chem. **98**, 2158 (1994).
- [7] N. A. Hill and K. B. Whaley, Phys. Rev. Lett. **75**, 1130 (1995); *ibid.* **76**, 3039 (1996).

- [8] C. Delerue, M. Lannoo, and G. Allan, Phys. Rev. Lett. **76**, 3038 (1996).
- [9] M. Lannoo, C. Delerue, and G. Allan, Phys. Rev. Lett. **74**, 3415 (1995); G. Allan, C. Delerue, M. Lannoo, and E. Martin, Phys. Rev. B **52**, 11 982 (1995).
- [10] M. S. Hybertsen and S. G. Louie, Phys. Rev. B **34**, 5390 (1986).
- [11] J. R. Chelikowsky, N. Troullier, and Y. Saad. Phys. Rev. Lett. **72**, 1240 (1994).
- [12] E. L. Briggs, D. J. Sullivan, and J. Bernholc, Phys. Rev. B **52**, R5471 (1995); F. Gygi and G. Galli, *ibid.*, R2229 (1995); G. Zumbach, N. A. Modine, E. Kaxiras, Solid State Commun. **99**, 57 (1996).
- [13] S. Ögüt, J. R. Chelikowsky, and S. G. Louie, Phys. Rev. Lett. **79**, 1770 (1997).
- [14] R. W. Godby and I. White, Phys. Rev. Lett. **80**, 3161 (1998); S. Ögüt, J. R. Chelikowsky, and S. G. Louie, *ibid.*, 3162 (1998).
- [15] M. Rohlfing and S. G. Louie, Phys. Rev. Lett. **80**, 3320 (1998); private communication.
- [16] N. Troullier and J. L. Martins, Phys. Rev. B **43**, 1993 (1991).
- [17] L. Kleinman and D. M. Bylander, Phys. Rev. Lett. **48**, 1425 (1982).
- [18] D. M. Ceperley and B. J. Alder, Phys. Rev. Lett. **45**, 566 (1980).
- [19] L. Brus, J. Phys. Chem. **90**, 2555 (1986); Y. Kayanuma, Phys. Rev. B **38**, 9797 (1988).
- [20] A. Franceschetti and A. Zunger, Phys. Rev. Lett. **78**, 915 (1997).
- [21] I. Vasiliev, S. Ögüt, and J. R. Chelikowsky, Phys. Rev. Lett. **78**, 4805 (1997).
- [22] G. Srinivasan, Phys. Rev. **178**, 1244 (1969).
- [23] S. Furukawa and T. Miyasato, Phys. Rev. B **38**, 5726 (1988).